Active Damping of Free-Rotor Gyroscopes during Initial Spin-Up

BRADFORD W. PARKINSON*
U.S. Air Force Academy, Colorado Springs, Colo.

AND

BENJAMIN LANGE†
Stanford University, Stanford, Calif.

The free-rotor gyro is so named because the nearly spherical gyrorotor is not mechanically constrained to rotate about a particular axis. Therefore, it may be initially spun up about any rotor fixed axis. As seen in the rotor, the subsequent motion of the angular velocity vector after spin-up is the well-known classical polhode motion about either the maximum or the minimum principal axes of inertia. The maximum axis of inertia is the desired spin axis direction because it is the only stable free-rotor spin direction in the presence of minute energy losses during flexures of the rotor. Consequently, the rotor-fixed markings used for spin axis readout of many of these gyros are referenced to the maximum axis of inertia. The principle delays in activating typical gyros are 1) waiting for a passive d.c. field to damp the gyro spin axis into the maximum axis of inertia of the rotor after it has been spun up (this requires typically five times the spin-up time) and 2) waiting for the thermal transient (of spin-up and damping) to subside. This paper describes a method of *actively* controlling the spin axis in the rotor, while leaving it unchanged with respect to a case-fixed reference. A control algorithm, called "Hemispheric Torquing" is used to *actively* damp the spin axis to the proper rotor fixed direction. It offers the advantage of being able to reduce damping times to less than is required for initial spin-up.

Introduction

FREE-ROTOR gyros require a spin-axis direction along the axis of maximum moment inertia of the rotor. This constraint arises in gyros which depend upon rotor-fixed markings for readout.

For most applications some scheme of artificially damping the spin axis to the maximum axis of inertia must be used. The passive method of applying a strong d.c. field parallel to the spin axis suffers because of the temperature transients it creates, and because the time required is large compared to the spin-up time and because either end of the rotor may come up. At Stanford an active damping scheme, which operates simultaneously with rotor spin-up, has been developed that can reduce these damping times to less than the time required for spin-up and can always make the same end come up. This solution was motivated by the Unsupported Gyro Development Program.[1,2]

The mechanization that we have conceived for damping in the large is called "Hemispheric Torquing." It is fairly simple in concept. The essential part of the scheme is to apply a torque whose average in inertial space is zero; but, because it switches in synchronization with the rotor rotation, it has a net effect when viewed in the rotor frame of reference. This net torque can be considered as a rectification in the rotor's coordinates. In effect, the angular rate of the rotor remains fixed in the laboratory while the rotor precesses beneath it to the desired axis.

As the spin axis of the rotor approaches the desired direction, Hemispheric Torquing will not work because the hemisphere sensor (which the scheme must use) tends to see both hemispheres at once. This latter phase of the active damping problem is termed fine erection, from the idea that we are erecting the spin axis to the maximum axis of inertia of the rotor.

This paper will deal with in-the-large damping, including a description of the hemispheric torquer and its equations of motion and the results of analog and digital simulations. The problem of fine erection has been solved, but it will be left to a future paper and only described here. The equations of motion and a control law based on frequency symmetry symmetry[3,5,6] ‡ have been formulated, and an error analysis performed.

Stanford is testing a model of the hemispheric torquer, and it has performed very well. The techniques of mechanization and the results will be discussed in a forthcoming paper.

Symbols and Notation

Vectors and second-order tensors are indicated by boldface type. A small letter directly below a quantity implies the quantity is a matrix of the coordinates of the vector or tensor in the axis set designated by the small letter (e.g., $\underset{i}{B}$ means the column matrix which represents vector **B** coordinated in frame i). Unit vectors will be designated as **1**.

Presented at the AIAA/JACC Guidance and Control Conference, Seattle, Wash., August 15–17, 1966 (no paper number; published in bound volume of conference papers); submitted March 10, 1967; revision received August 13, 1969. The research reported here is part of a program supported at Stanford University by the U.S. Air Force under Contract AF33(615)-1411 from the Air Force Avionics Laboratory. This work is part of B. Parkinson's doctoral thesis.

* Member of the Faculty; Lt. Colonel U.S. Air Force. Member AIAA.

† Associate Professor, Department of Aeronautics and Astronautics. Member AAIA.

‡ Frequency symmetric is defined as follows: Any linear constant system of even order, $2n$, which possesses the following property will be said to be frequency symmetric:

There exists a linear constant system of one-half the order of the original system, n, whose characteristic roots will exactly duplicate the characteristic roots of the original system if they are translated parallel to the imaginary axis in the complex plane up and down by distances $\pm j\omega_s$. A symmetric body rotating about an axis which is close to the axis of symmetry has this property.

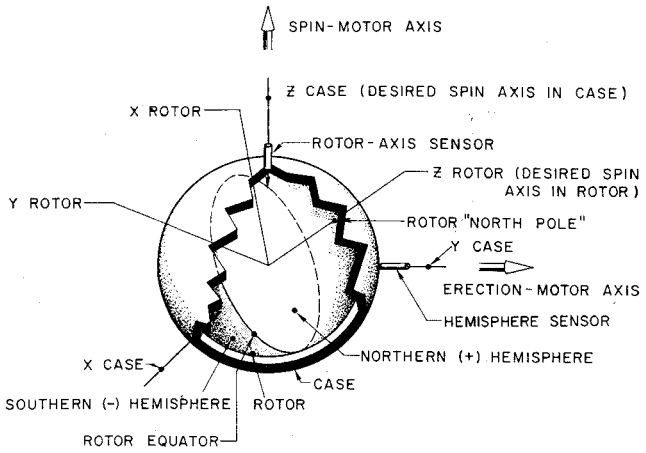

Fig. 1 Schematic view of the rotor and case.

Coordinate transformations will be designated with a T and the subscript a/c will indicate "axis set a with respect to c," e.g., $\underset{g}{B} = T_{a/c}\underset{c}{B}$.

Vector derivatives with respect to time are designated by a small letter over the vector; the letter designated the frame in which the derivative is to be taken (e.g., $\overset{c}{\mathbf{B}}$ = the derivative with respect to time of vector $\mathbf{B}$ in frame c). Since $\overset{c}{\mathbf{B}}$ is again a vector, the rule for coordinatizing still holds, e.g., $\underset{d}{\overset{c}{B}}$ is column matrix representing the coordinates of the vector derivative referred to frame c, the coordinates being in frame d.

A frequently used quantity in vector kinematics is the angular rate vector. An example of this would be: $\mathbf{W}^{a-c} \triangleq$ the angular rate of frame a with respect to c. For the coordinatizing of the cross product, which can be represented as an antisymmetric matrix, a frequently used notation will be $\left[\underset{b}{W^{a-c}}\times\right]$ to represent the matrix,

$$\begin{bmatrix} 0 & -W_z & W_y \\ W_z & 0 & -W_x \\ -W_y & W_x & 0 \end{bmatrix} a-c \text{ in the } b \text{ frame}$$

Damping in the Large: Hemispheric Torquing

A. Description of the Hemispheric Torquer

The typical free-rotor gyro consists of a hollow case, which contains a hermetically sealed spherical cavity and, inside the cavity, an almost spherical rotor (or ball) on which are markings to permit the readout of the rotor spin-axis direction. To activate the device the rotor must be levitated, and then spun-up. If the rotor spin direction is considered as a vector, this vector must have a prespecified direction in the case (so the device measures the proper angular motion) and also in the rotor§ (so the readout scheme will work). Before proceeding, the applicable coordinate frames shall be described.

There are three coordinate frames to be considered in this description. The first is fixed to the case (and hence called the case coordinate system) and assumed to be rotating, if at all, very slowly in inertial space and hence is called the i-frame. Attached to this frame is a hemisphere sensor capable of determining which ball hemisphere is opposite a fixed point on the case, the spin-up coils, the erection coils (which probably would be identical to the spin-up coils), and a rotor-axis sensor that can read a marking on the rotor in two coordinates (the location of the marking will be further described later) when it is in the field of view. The location of these two sensors will be described after considering the second coordinate system.

A second coordinate frame (the b-frame) is attached to the rotor (or ball). The z axis of the coordinate system is along an axis from the center of the rotor towards the desired rotor spin direction. Located at the intersection of this z axis and the rotor surface is the marking to be sensed by the rotor-axis sensor. Perpendicular to the z axis are located the x and y axes; they determine a plane which passes through the center of the rotor and intersects the rotor surface at the rotor equator. This equator divides the rotor into two hemispheres: the northern and southern in analogy to the earth. The north pole is the rotor z axis which is also the desired rotor spin axis.

The third coordinate frame (the floating or f-frame) has its z axis aligned with the rotor angular velocity and its y axis in the xy plane of the b-frame.

Returning to the location of the sensors in the case, if the rotor is spinning about the rotor z axis and also is spinning about the desired axis in the case, the rotor-axis sensor, located on this spin axis in the case, will be reading (0,0), that is, it will read, in two coordinates, the null position. Also, the hemisphere sensor will be located in the case opposite the rotor equator. Its output will be indeterminate since its field of view will include both hemispheres.

Figure 1 shows the rotor case in a schematic view. The spin-up of a free-rotor gyro is accomplished by applying a rapidly spinning magnetic field that rotates about an axis fixed to the outer case of the instrument. (This field creates a torque in the manner of the squirrel cage induction motor.) It is about this axis (called the spin-motor axis) that the ball tends to spin, when viewed in the case coordinate system. The spin-motor axis nominally passes through the rotor-axis sensor (the effect of misalignment will be considered by the fine erection analysis). The motor field and perhaps an additional magnetic field parallel to the spin-motor axis tends to cage the spin vector in the case. That is, the rotor will have its spin axis very close to the desired direction in the case.

Unfortunately, in most instances, the spin axis will be misaligned (by as much as 180°) in the rotor. The scheme for moving the spin axis in the rotor while leaving it virtually undisturbed in the case coordinates is called hemispheric torquing. It will now be described and heuristically justified: the rigorous justification must rest with the derivation and results of the dynamical equations in the next section.

Assume the rotor is caged to the proper axis in the case but rotating about an axis at 45° north latitude in the rotor coordinate system. The hemisphere sensor will sense the north (+) hemisphere and then one-half rotor cycle later will sense the south (−) hemisphere. An erection-motor axis is

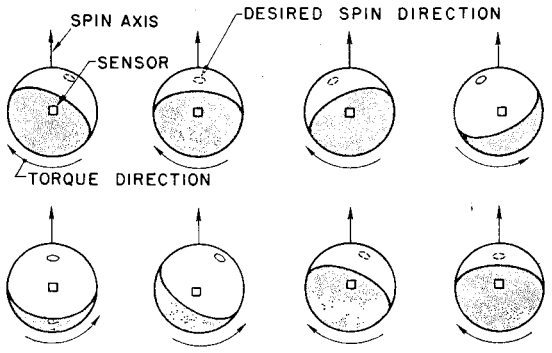

Fig. 2 Successive views of rotor during hemispheric torquing.

§ The desired direction in the rotor is along the maximum axis of inertia which is the only stable free rotor spin direction (in the presence of damping) due to a minute energy loss during small flexures of the nonrigid rotor.

defined about which a spinning magnetic field will rotate to create an erection torque. This erection-motor axis is fixed in the case and is paralle to the hemisphere-sensor axis, passing through the center of the cavity. Let the spin-motor axis be the case z axis, the erection-motor axis be the case y axis and the hemisphere sensor also be on the case y axis.

The rule for active damping is to apply a plus erection torque when the northern hemisphere is sensed and a minus erection torque when the southern hemisphere is sensed. This is, of course, the source of the name hemispheric torquing. For the method to work there is an upper limit $(M_e)/(|W^{b-i}|^2)$ of about 0.1 where M_e is a normalized erection torque in rad/sec^2 and W^{b-i} is the rotor (or ball) angular rate in (rad/sec). When this restriction holds, the spin direction will be only slightly deflected from the spin-motor axis during erection. The positive and negative torquing times will be very nearly equal and there will be no net angular momentum imparted to the rotor by the erection motor.

Returning to our example at 45° latitude, the sequence of drawings in Fig. 2 shows the action as the rotor spins. Note that the torque is of a sense to always urge the angular rate towards the rotor z axis. This effect is like a phase sensitive demodulation of an a.c. signal to produce a rectified value.

This hemispheric torquing scheme will work as long as the two hemispheres can be differentiated by the sensor. When this is no longer true, the active damper must switch to the fine erection phase which employs the rotor-axis sensor.

The hemispheric torquing scheme, which depended on the spin axis being roughly along the case z axis, will no longer work when the spin-axis misalignment in the rotor is the same order of magnitude as the angular difference between spin axis and case z axis. This effect occurs at roughly the same time the hemisphere sensor has difficulty, so no additional problems are imposed.

B. Equations of Motion for Hemispheric Torquing

The derivation of these equations of motion considers an initially rotating, almost spherical rotor, whose spin axis is very nearly along a desired inertial direction, but which is displaced from the desired z axis of the rotor. Figure 3 shows the coordinate geometry and Fig. 4 shows typical torque time histories. The inertially fixed direction of the spin-up motor axis is along the vector $\mathbf{N}$. The floating frame is attached to the angular rate vector $\mathbf{W}^{b-i}$. Although this may seem to be an awkward coordinate system, it is necessary because $\mathbf{W}^{b-i}$ and $\mathbf{N}$ are not colinear. N_x and N_y are the x and y components of $\mathbf{W}$ in the f-frame. The angles D and E define the direction of $\mathbf{W}^{b-i}$ in the rotor. In terms of these variables, the object of the hemispheric torquer is to drive E

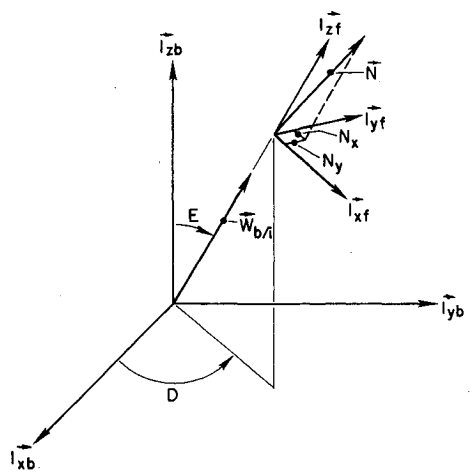

Fig. 3 Definitions of coordinate frames and variables.

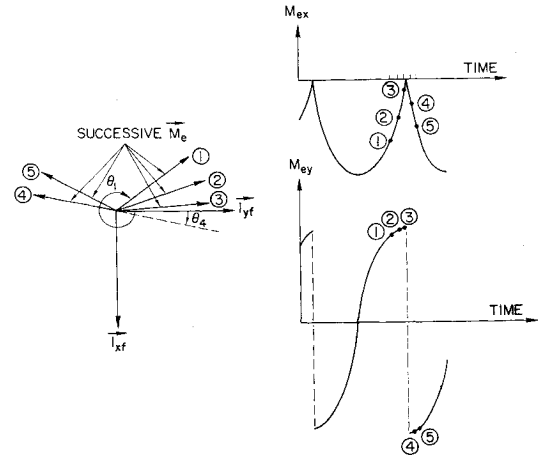

Fig. 4 Successive torque directions and components in the f frame.

to 0 and to make $\mathbf{W}$ parallel to $\mathbf{N}$. The transformation from frame b to f is¶

$$T_{f/b} = \begin{bmatrix} cCcE & sDcE & -sE \\ -sD & cD & 0 \\ cDsE & sDsE & cE \end{bmatrix}$$

Let the moment of inertia tensor in the rotor be

$$\underset{b}{I_b} \triangleq I_z \begin{bmatrix} (1-\epsilon_1) & 0 & 0 \\ 0 & (1-\epsilon_2) & 0 \\ 0 & 0 & 1 \end{bmatrix}$$

where ϵ_1 and ϵ_2 are small quantities reflecting the unequal principal moments of inertia.

The basic vector moment equation is

$$\mathbf{M} = \overset{i}{\mathbf{H}} = \overset{b}{\mathbf{H}} + \mathbf{W}^{b-i} \times \mathbf{H}$$

or since $\mathbf{H} = \mathbf{I}_b \cdot \mathbf{W}^{b-i}$ and $\overset{b}{\mathbf{I}}_b = 0$

$$\mathbf{M} = \mathbf{W}^{b-i} \times \mathbf{I}_b \cdot \mathbf{W}^{b-i} + \mathbf{I}_b \cdot \overset{b}{\mathbf{W}}^{b-i} \tag{1}$$

where $\mathbf{H}$ = angular momentum, and $\mathbf{M}$ = applied moment on the ball

The basic plan of attack is to coordinatize Eq. (1) in frame f, solve for $\underset{f}{\overset{b}{W}}{}^{b-i}$ and interpret the result in terms of $\dot{D}$, $\dot{E}$, and $\dot{W}$. The following relations follow from the definitions and Fig. 3:

$$\underset{f}{W}{}^{b-i} = \begin{bmatrix} 0 \\ 0 \\ W \end{bmatrix}, \quad \underset{f}{W}{}^{f-b} = \begin{bmatrix} -\dot{D}sE \\ \dot{E} \\ \dot{D}cE \end{bmatrix}$$

$$\overset{b}{W}{}^{b-i} = \overset{f}{W}{}^{b-i} + \begin{bmatrix} W^{f-b} \\ f \end{bmatrix} \times \underset{f}{W}{}^{b-i} =$$

$$\begin{bmatrix} 0 \\ 0 \\ \dot{W} \end{bmatrix} + \begin{bmatrix} -\dot{D}sE \\ \dot{E} \\ \dot{D}cE \end{bmatrix} \times \begin{bmatrix} 0 \\ 0 \\ W \end{bmatrix}$$

$$\underset{f}{\overset{b}{W}}{}^{b-i} = \begin{bmatrix} 0 & W & 0 \\ WsE & 0 & 0 \\ 0 & 0 & 1 \end{bmatrix} \begin{bmatrix} \dot{D} \\ \dot{E} \\ \dot{W} \end{bmatrix} \tag{2}$$

inverting

$$\begin{bmatrix} \dot{D} \\ \dot{E} \\ \dot{W} \end{bmatrix} = \begin{bmatrix} 0 & (WsE)^{-1} & 0 \\ W^{-1} & 0 & 0 \\ 0 & 0 & 1 \end{bmatrix} \underset{f}{\overset{b}{W}}{}^{b-i} \tag{3}$$

¶ Here and after $cD \triangleq \cos D$, $sD \triangleq \sin D$, etc.

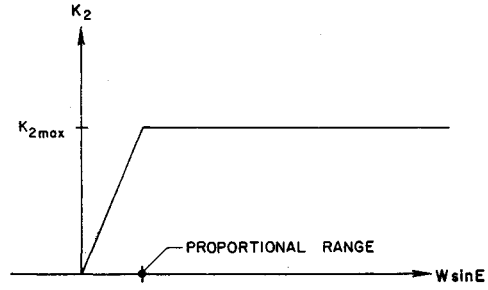

Fig. 5 Torque vs WSE.

From Eq. (1)

$$\overset{b}{\underset{f}{W}}{}^{b-i} = T_{f/b}\left[\underset{b}{I_b}\right]^{-1}\left\{\underset{b}{M} - \left[\underset{b}{W^{b-i}}\times\right]\underset{b}{I_b}\underset{b}{W^{b-i}}\right\} \tag{4}$$

Using the definition of $\underset{b}{I_b}$:

$$\left[\underset{b}{I_b}\right]^{-1} = \frac{1}{I_z}\{[U] + [\mathcal{E}]\} \tag{5}$$

where

$$[\mathcal{E}] = \begin{bmatrix} \epsilon_1/(1-\epsilon_1) & 0 & 0 \\ 0 & \epsilon_2/(1-\epsilon_2) & 0 \\ 0 & 0 & 0 \end{bmatrix}$$

where $[U]$ is the 3×3 identity matrix. Using Eq. (5) in Eq. (4)

$$\overset{b}{\underset{f}{W}}{}^{b-i} = \left[\frac{1}{I_z}T_{f/b}\underset{b}{M} - T_{f/b}\left[\underset{b}{W^{b-i}}\times\right]\left(\frac{\underset{b}{I_b}}{I_z}\right)\underset{b}{W^{b-i}}\right] + T_{f/b}[\mathcal{E}]\left[\left(\frac{\underset{b}{\mathbf{M}}}{I_z}\right) + \left[\underset{b}{W^{b-i}}\times\right]\left(\frac{\underset{b}{I_b}}{I_z}\right)\underset{b}{W^{b-i}}\right] \tag{6}$$

The second term of Eq. (6) is of the magnitude of the epsilons relative to the first which makes it typically 10^{-3} or less than the first. It will be discarded.** The sources of external torque are as follows.

1. *Spin-up*††

$(1/I_z)\mathbf{M}_{su} \triangleq K_1\mathbf{N}$ where K_1 = const, and is a function of rotor material field strength, spin-up frequency, etc.

2. *Damping torque*‡‡

$$(1/I_z)\mathbf{M}_d \triangleq -K_3\mathbf{N} \times (\mathbf{W}^{b-i} \times \mathbf{N})$$

This is due to an applied magnetic field in the $\mathbf{N}$ direction. The torque magnitude is proportional to the angular rate perpendicular to $\mathbf{N}$.

3. *Erection torque*

The erection torque is assumed to be a saturation function of E with a small proportional range as shown in Fig. 5. The small proportional range is assumed for convenience in integration, since the erection scheme would be switched to fine erection before that point is reached. The torque is assumed to be in the $\mathbf{I}_{xf}$, $\mathbf{I}_{yf}$ plane.§§ Relative to the rotor it rotates at $\mathbf{W}^{i-b} = -\mathbf{W}^{b-i}$ and switches signs so as to always have a negative $\mathbf{1}_{xf}$ component.

Let

$$\theta \triangleq \int_0^t \mathbf{W}^{b-i}\cdot\mathbf{N}d\tau = \int_0^t WN_z d\tau$$

then successive positions of $\mathbf{M}_e$ in the $\mathbf{1}_{xf}$, $\mathbf{1}_{yf}$ plane are shown in Fig. 4. Let¶¶

$$\theta^* \triangleq \theta \bmod \pi$$

Then

$$\frac{\underset{f}{M_e}}{I_z} = \begin{bmatrix} K_2\theta S^* \\ -K_2 c\theta^* \\ 0 \end{bmatrix}$$

where K_2 is the normalized torque magnitude. For larger angles (E) the magnitude is constant, but as E becomes small it becomes proportional to E.* Eq. (6), with the various torques included, becomes

$$\overset{b}{\underset{f}{W}}{}^{b-i} = \begin{bmatrix} K_1N_x + K_3WN_zN_x - K_2S\theta^* \\ K_1N_y + K_3WN_zN_y - K_2c\theta^* \\ K_1N_z - K_3W(N_x^2 + N_y^2) \end{bmatrix} + -T_{f/b}\left[\underset{b}{W^{b-i}}\times\right]\left\{[U] + \begin{bmatrix} -\epsilon_1 & 0 & 0 \\ 0 & -\epsilon_2 & 0 \\ 0 & 0 & 0 \end{bmatrix}\right\}\underset{b}{W^{b-i}}$$

$$\overset{b}{\underset{f}{W}}{}^{b-i} = \begin{bmatrix} K_1N_x + K_3WN_zN_x - S\theta^* \\ K_1N_y + K_3WN_zN_y - K_2c\theta^* \\ K_1N_z - K_3W(N_x^2 + N_y^2) \end{bmatrix} + W^2\begin{bmatrix} MSESDcD \\ LSEcE \\ 0 \end{bmatrix}$$

where $M \triangleq \epsilon_1 - \epsilon_2$, $L \triangleq S^2D\epsilon_2 + c^2D\epsilon_1$. Using Eq. (3)

$$\begin{bmatrix} \dot{D} \\ \dot{E} \\ \dot{W} \end{bmatrix} = \begin{bmatrix} \dfrac{K_1N_y}{WSE} + \dfrac{K_3N_yN_z}{SE} + LWcE - \dfrac{K_2c\theta^*}{WSE} \\ \dfrac{K_1N_x}{W} + K_3N_zN_x - \dfrac{K_2S\theta^*}{W} + MWSESDcD \\ K_1N_z - K_3W(N_x^2 + N_y^2) \end{bmatrix} \tag{7}$$

The derivatives of $\mathbf{N}$ are found

$$\overset{f}{\mathbf{N}} = \overset{i}{\mathbf{N}} - \mathbf{W}^{f-i} \times \mathbf{N}, \quad \overset{i}{\mathbf{N}} = 0 \text{ (by definition)}$$

$$\underset{f}{W}{}^{f-i} = \underset{f}{W}{}^{f-b} + \underset{f}{W}{}^{b-i}$$

so by the definitions of Eq. (2)

$$\dot{N}_x = -\dot{E}N_z + (W + \dot{D}cE)N_y$$

$$\dot{N}_y = -(W + \dot{D}cE)N_x - \dot{D}N_zSE \tag{8}$$

and the N_z derivative is second order small for N_x, N_y small,

** Its size is probably the same as that of the torquing rate uncertainty in a typical erection scheme. For the ESG, ϵ on the order of 0.1 has been simulated using the exact Eq. (6). The hemispheric torquer still performed satisfactorily; the main effect of the large ϵ was to increase the azimuth angle (D) during torquing. The damping time was increased by less than a factor of two depending on initial N_x and N_y.

†† The spin-up is assumed due to a rotating magnetic field which is at a much higher frequency than the angular rate of the ball. It is not germane to this paper to discuss the boundary value problem associated with magnetic eddy current torquing. The assumption here is that the angular acceleration due to this torque is effectively constant for the duration of the problem. Lange[2] discusses the problem for the special cases of a silicon rotor.

‡‡ Again the details of eddy current damping are not to be considered here. The assumption is that a d.c. or slowly varying a.c. field whose axis is along the direction of the spin-motor axis will cause a damping torque which opposes and is proportional to spin components perpendicular to the field axis.

§§ Since N_x and N_y are small, there is a negligible component of K_2 along $\mathbf{1}_{zf}$.

¶¶ A mod $B = A - nB$ for the largest integer n that makes the quantity ≥ 0.

* Note that E cannot be negative.

N_z is found from

$$N_z = (1 - N_x^2 - N_y^2)^{1/2} \tag{9}$$

The equations of motion are Eqs. with

$$\theta^* = \left[\int_0^t WN_z d\tau\right] \bmod \pi$$

These equations have been programed and run on the digital computer, but because they are very time consuming,† a better technique for their solution will be sought.

Rather than place these equations in normalized form, the next section will develop a more valuable description of the system using a modified Kryloff-Bogoliuboff (KB) technique.

C. Method of Kryloff-Bogoliuboff Applied to the Hemispheric Torquing Equations

Kryloff and Bogoliuboff[5] have formalized a number of techniques for eliminating the high-frequency oscillation from dynamical equations. In this section a variation of the "Theory of the First Approximation" will be applied to eliminate the high-frequency components in N_x and N_y which appear when the hemispheric torquing equations are solved on the digital computer.

Using the definitions of the last section, the equations to be solved are Eqs. (7–9). Assume that‡

$$N_x(t) = N_{x0}(t) + A(t)\sin[rt - l(t)]$$
$$N_y(t) = N_{y0}(t) + A(t)\cos[rt + l(t)]$$

where

$$r = W + LWc^2E - K_2(c\theta^* cE/W\$E)$$

The selection for r is made because this term appears in the equations in the symmetrical form typical of a frequency. Then

$$\dot{N}_x(t) = \dot{N}_{x0} + \dot{A}\sin(rt + l) + A\cos(rt + l)(r + \dot{l} + \dot{r}t)$$
$$\dot{N}_y(t) = \dot{N}_{y0} + \dot{A}\cos(rt + l) - A\sin(rt + l)(r + \dot{l} + \dot{r}t)$$

After inserting these and Eq. (7) into Eq. (8) and simplifying§

$$\dot{N}_{x0} + \dot{A}\sin(rt + l) + A\cos(rt + l)(\dot{l} + \dot{r}t) - rN_{y0} = (K_1/W + K_3N_x)\cdot\{-N_{x0}N_z - A\sin(rt + l)N_z + (cE/\$E)[N_{y0}^2 + 2N_{y0}A\cos(rt + l) + A^2\cos^2(rt + l)]\} + K_2(N_z\$\theta^*/W) + W\$EN_z\$DcD(\epsilon_1 - \epsilon_2) \tag{10}$$

$$\dot{N}_{y0} + \dot{A}\cos(rt + l) - A\sin(rt + l)(\dot{l} + \dot{r}t) + N_{x0}r = (K_1/W + K_3N_z)\cdot\{-N_{y0}N_z - A\cos(rt + l)N_z - (cE/\$E)[N_{x0}N_{y0} + N_{x0}A\cos(rt + l) + N_{y0}A\sin(rt + l) + A^2\sin(rt + l)\cos(rt + l)]\} + K_2N_zc\theta^*/W - LW\$EcEN_z \tag{11}$$

Now for auxiliary conditions let

$$\dot{N}_{x0} - rN_{y0} = \left(\frac{K_1}{W} + K_3N_z\right)\left(-N_{x0}N_z + \frac{cE}{\$E}N_{y0}^2\right) + \frac{K_2N_z\$\theta^*}{W} - WN_z\$DcD(\epsilon_1 - \epsilon_2)\$E \tag{12}$$

$$\dot{N}_{y0} + rN_{x0} = \left(\frac{K_1}{W} + K_3N_z\right)\left(-N_{y0}N_z - \frac{cE}{\$E}N_{x0}N_{y0}\right) + \frac{K_2N_zc\theta^*}{W} - WN_z\$EcE(cD^2\epsilon_2 + cD^2\epsilon_1) \tag{13}$$

N_{x0} and N_{y0} at the initial time can be adjusted so $\dot{N}_{x0}$ and $\dot{N}_{y0}$ are zero. This adjustment effectively throws the initial condition into A and l. Also, these equations are to be averaged over one cycle of $\cos(rt + l)$.¶ This eliminates the θ^* term and replaces it with its average value. Inserting Eqs. (12) and (13) into Eqs. (10) and (11) and solving for $\dot{l}$ and $\dot{A}$,

$$\begin{bmatrix}\dot{l}\\ \dot{A}\end{bmatrix} = \left(\frac{K_1}{W} + K_3N_z\right)\begin{bmatrix}\left\{\left(\frac{cE}{\$E}\right)[N_{y0}(2c^2P + \$^2P) + N_{x0}cP\$P + AcP]\right\}\\ \left(-AN_z + \frac{cE}{\$E}[N_{y0}A\$PcP - A^2\$P - N_{x0}Ac^2P]\right)\end{bmatrix}\begin{bmatrix}\dot{r}t\\ 0\end{bmatrix} \tag{14}$$

where $P \triangleq rt + l$ is the phase angle.

Now if Eq. (14) is averaged over one period (2π on P) the result is the average derivative

$$\begin{bmatrix}\langle\dot{l}\rangle\\ \langle\dot{A}\rangle\end{bmatrix} = \left(\frac{K_1}{W} + K_3N_z\right)\begin{bmatrix}\frac{cE}{\$E}\frac{3N_{y0}}{2}\\ -AN_z - \frac{cE}{\$E}\frac{N_{x0}A}{2}\end{bmatrix} - \begin{bmatrix}\dot{r}t\\ 0\end{bmatrix} \tag{15}$$

Inserting the assumed form for N_x and N_y into Eq. (7) and also forming the average derivative,

$$\langle\dot{D}\rangle = (K_1/W + K_3N_z)N_{y0}/\$E + LWcE \tag{16}$$
$$\langle\dot{E}\rangle = (K_1/W + K_3N_z)N_{x0} - 2K_2/W\pi + MW\$DcD\$E \tag{17}$$
$$\langle\dot{W}\rangle = K_1[1 - \tfrac{1}{2}(N_{x0}^2 + N_{y0}^2 + 2A^2)] - K_3W(N_{x0}^2 + N_{y0}^2 + 2A^2) \tag{18}$$

At this point terms involving products of N_{x0}, N_{y0}, and A may be discarded.**

† The problem of long running time was due to the high-frequency components in N_x and N_y.

‡ One is free to assume the solution to be in any form that is convenient. We have assumed this form because it roughly fits the digital data with N_{x0}, N_{y0}, and A slowly varying quantities. Note that there are four independent quantities, so two auxiliary conditions are yet to be specified.

§ The formula $N_z^2 = 1 - N_x^2 - N_y^2$ reduces to $N_z^2 = 1 - N_{x0}^2 - N_{y0}^2 - 2A[N_{x0}\sin(rt + l) + N_{y0}\cos(rt + l)] - 2A^2$. Since the variables N_{x0}, N_{y0}, and A are small $N_z = 1 - \frac{1}{2}(N_{x0} + N_{y0}) + 2A[N_{x0}\sin(rt + l) + N\cos(rt + l) + 2A^2]$.

¶ The assumption is that E, D, N_{x0}, and N_{y0} are slowly varying quantities.

** These quantities are usually very small, but later a condition will be given that insures their being less than 0.1, which means that errors are less than 0.01 at the very worst. Typically the error is closer to the order of 10^{-6}. As $\$E \to 0$, $cE/\$E \to \infty$ but N_{x0} and N_{y0} are also $\to 0$. Integration on the digital computer reveals that none of these derivatives blow up. That is, $N_{y0}/\$E \to 0$. This problem is not significant because the active damper must be switched to the fine erection mode as E goes to 0.

Performing the averaging Eqs. (12) and (13),

$$\langle \dot{N}_{x0} \rangle = \hat{r} N_{y0} + (K_1/W + K_3)(-N_{x0}) - W \S D c D(\epsilon_1 - \epsilon_1) \S E \quad (19)$$

$$\langle \dot{N}_{y0} \rangle = -\hat{r} N_{x0} + (K_1/W + K_3)(-N_{y0}) + 2K_2/\pi W - W \S E c E(\S D^2 \epsilon_2 + c D^2 \epsilon_1) \quad (20)$$

where

$$\hat{r} = W + W c^2 E(\S^2 D \epsilon_2 + c^2 D \epsilon_1)$$

Let $\hat{W} = W/W_0$ where W_0 is the value at $t = 0$.

Including first-order terms from Eq. (18); $\hat{W} = K_1/W_0$. Let $\tau = W_0 t$ be the nondimensional time, then

$$\langle d\hat{W}/d\tau \rangle = K_1/W_0^2 \triangleq P_1 \quad (21)$$

Again using nondimensional time and the definition of $\hat{r}$, Eqs. (19) and (20) become

$$\langle dN_{x0}/d\tau \rangle = [\hat{W}(1 + Lc^2E) - P_2{}^2 c D/(\pi \hat{W} \S E)] N_{y0} + (P_1/\hat{W} + P_3)(-N_{x0}) - M \hat{W} \S D c D \S E \quad (22)$$

$$\langle dN_{y0}/d\tau \rangle = -[\hat{W}(1 + Lc^2E) - P_2{}^2 c E/(\pi \hat{W} \S E)] N_{x0} + (P_1/\hat{W} + P_3)(-N_{y0}) + P_2 2/\pi - LW \S E c E \quad (23)$$

$$\langle dD/d\tau \rangle = (P_1/\hat{W} + P_3) N_{y0}/\S E + L \hat{W} c E \quad (24)$$

$$\langle dE/d\tau \rangle = (P_1/\hat{W} + P_3) N_{x0} - P_2 2/\pi \hat{W} + M \hat{W} \S D c D \S E \quad (25)$$

where

$$P_1 \triangleq K_1/W_0^2,\ P_2 \triangleq K_2/W_0^2,\ P_3 \triangleq K_3/W_0,\ \tau \triangleq W_0 t \quad (26)$$

Equations (22–25) represent the gyro system when hemispheric torquing is applied. This set is called the KB equations. After the length of the development it was felt necessary to validate the assumptions that were made. This was done by simultaneously running the exact equations and successive approximations down to the last set on the digital computer. The goal of the control is to drive E to 0. A comparison of all results in E was overplotted for possible inclusion here, but because the results were so close they plotted as one line. Numerically the differences are shown in Table 1.

These values were computed for $P_1 = 0.0065$, $P_2 = 0.00040$, $P_3 = 0.0100$, $\epsilon_1 = -0.00001$, and $\epsilon_2 = -0.00001$.

D. Estimation of the Erection Time

By differentiating Eq. (22) and combining it with Eq. (23) to eliminate N_{y0} and its derivatives the following equation for N_{x0} may be derived††:

Table 1 Comparison of exact and KB equations

	Coelevation (E), rad	
τ, sec	Exact	Final KB approximation
0	0.10000	0.10000
50	0.08767	0.08760
100	0.07563	0.07558
150	0.06393	0.06392

†† All derivatives are with respect to τ.

$$\frac{d}{d\tau}(\langle \dot{N}_{x0} \rangle) + \left[\frac{P_1}{1 + P_1\tau} + P_3\right]\langle \dot{N}_{x0} \rangle + \left[-\frac{P_1{}^2}{(1 + P_1\tau)^2} + (1 + P_1\tau)^2 + P_3 P_1 + P_3{}^2(1 + P_1\tau)\right] N_{x0} = \frac{2}{\pi} P_2$$

If we only consider the steady-state solution to the equation and assume that P_3, $P_1 \leq 0.1$, an approximate solution is‡‡

$$N_{x0} = (2/\pi) P_2/(1 + P_1\tau)^2$$

This can be inserted in the Eq. (25) for $\langle \dot{E} \rangle$ and the result integrated to yield an approximate solution for E§§

$$E = E_0 - \frac{P_2}{P_1}\frac{2}{\pi}\left\{\ln(1 + P_1\tau) + P_3\left[\frac{1}{1 + P_1\tau} - 1\right] + \frac{P_1}{2}\left[\frac{1}{(1 + P_1\tau)^2} - 1\right]\right\} \quad (27)$$

This approximation was compared with the numerical integration of the KB equations. The results were essentially identical and are tabulated in Ref. 7, p. 42.

At this point it is worthwhile to summarize the notation of Eq. (27). If W_0 = rotor spin (rad/sec) at initiation of hemispheric torquing then:

$$P_1 = \frac{\text{angular acceleration due to spin motor}}{W_0{}^2}, \frac{\text{rad}}{\text{sec}^2}$$

$$P_2 = \frac{\text{angular acceleration due to erection motor}}{W_0{}^2}, \frac{\text{rad}}{\text{sec}^2}$$

$$P_2 = \frac{\text{angular acceleration due to passive damping}}{W_0}, \frac{\text{rad/sec}^2}{\text{rad/sec}}$$

$\tau = W_0 t$ dimensionless time

E, E_0 = coelevation angle, rad

It is a noteworthy result of our simulations that P_2 must be less than 0.1 or the requirements for P_3 become excessive. This is because a large P_2 tends to drive the spin direction too far away from the spin-motor axis (which would lead to the failure of the hemispheric torquer) unless a large damping field is present.

To obtain an approximation for the time required, Eq. (27) is approximately¶¶

$$E = E_0 - (P_2/P_1)(2/\pi) \ln(1 + P_1\tau)$$

which can be solved for τ

$$W_0 t = \tau = \frac{\exp[(E_0 - E)(P_1/P_2)\pi/2] - 1}{P_1}$$

and converting to the original K parameters Eq. (26)

$$t_e = \frac{W_0}{K_1}\left\{\exp\left[-\left(\pi \frac{\Delta E}{E}\frac{K_1}{K_2}\right)\right] - 1\right\} \quad (28)$$

‡‡ A slightly more accurate approximation is available if the terms involving $P_3{}^2$, $P_1{}^2$, $P_3 P_1$ are not neglected, but the present approximation is so good that it does not seem worthwhile to present the order.

§§ The ellipticity terms have been discarded. Their main effect is to change D; they represent torque levels that are significant for the free gyro but not for the system when undergoing erection.

¶¶ The parameters P_1 and P_3 are assumed to be small.

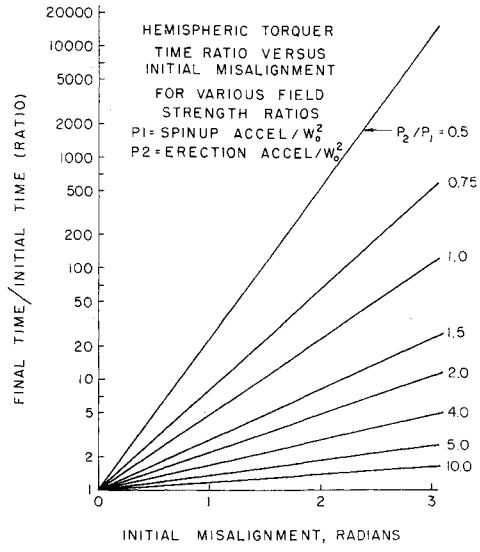

Fig. 6 Time ratio vs initial misalignment.

Where $\Delta E \triangleq$ change in coelevation (should be negative), and t_c = the time required.

If the spin field is turned on at $t = 0$ with the spin acceleration of K_1, then the initiation time (t_i) for hemispheric torquine is $t_i = W_0/K_1$.

The total running time up to erection is $t_f = t_i + t_e$. Using these definitions, Eq. (28) becomes

$$\frac{t_f}{t_i} = \exp\left(-\pi \frac{\Delta E}{2} \frac{K_1}{K_2}\right) \equiv \exp\left(-\pi \frac{\Delta E}{2} \frac{P_1}{P_2}\right) \quad (29)$$

If $\Delta E = -E_0$ so the final value of E is 0, the time ratio may be determined as shown in Fig. 6. The worst case is for a coelevation of π, so the longest final time is approximately

$$t_f = t_i \exp[-(\{\pi^2/2\}\ P_1/P_2)] \quad (30)$$

This result is shown in Fig. 7. Several values of P_1 with $P_1/P_2 = K_1/K_2 = \frac{1}{2}$ were checked against the KB results. Since the effect of P_1 and P_3 for Eq. (1) are not included, some error is expected when these values are large. The results are shown in Table 2. Thus, for large values of P_1, the Eq. (30) is about 10% optimistic.

If $W_0 \triangleq K_1 t_i$ then $P_1 \triangleq K_i/W_0^2 = 1/(W_0 t_i) \triangleq 1/\tau_i$, so a large P_1 corresponds to a small τ_i. The error in τ_f is as follows:

$$\text{error } (\tau_f) = \tau_i \cdot \text{error } (\tau_f/\tau_i)$$

Since τ_i is small, the absolute error in τ_f is also small. In other words the largest relative error in the approximation occurs for the case of erection being completed the fastest. Fortunately, this means the erection is completed long before the completion of spin-up, so the effect of the error is also the least.

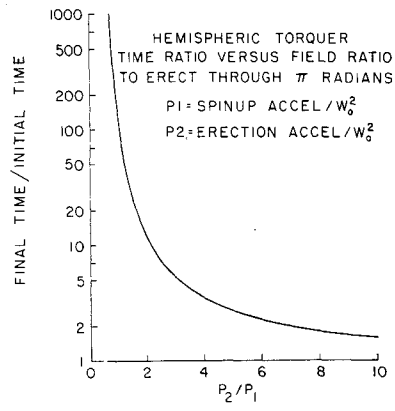

Fig. 7 Maximum time to erect for various field strength ratios.

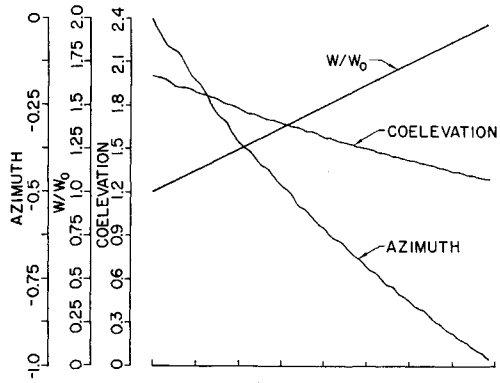

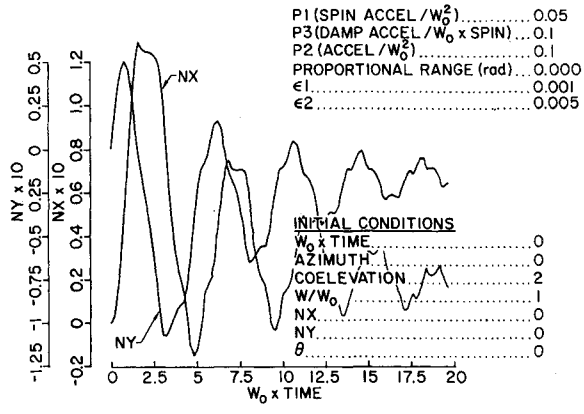

Fig. 8 Results using exact equations ($E_0 = 2.0$).

An example

Consider a gyro whose final spin rate is 12,000 rpm which can be attained in 10 min;

$$K_1 = 2 \text{ rad/sec}^2$$

Let the spin acceleration be reduced (until the erection phase is completed) to 1 rad/sec², and let $K_2 = 2$ rad/sec.² Erection may be initiated when $P_2 = K_2/W_0^2 \leq 0.1$, i.e., $W_0^2 \geq 10\ K_2$. Choose an W_0 of 5 rad/sec which corresponds to starting hemispheric torquing 5 sec after starting spin-up. Since $K_2/K_1 = 2$, for the worst case of π rad [from Eq. (30)] $t_f/t_i = 11.8$ so $t_f/t_i = 5 \times 11.8 = 59$ sec. At this point, the spin acceleration would be increased to 2 rad/sec² and the spin-up process continued until final spin rate is reached at about 10 min 30 sec. If the gyro could stand the power input of a K_2 of 4 rad/sec², the spin-up and erection process could be completed in ten minutes.* (If $W_0 = 7$ rad/sec then

Table 2 Comparison of exact and analytical expression for damping times

P_1	P_2	P_3	t_f/t_i from Eq. (36)	t_f/t_i actual integration
0.05	0.10	0.10	11.8	13.5
0.005	0.01	0.01	11.8	11.9
0.0005	0.001	0.001	11.8	11.8

* The spin acceleration would not have to be reduced to 1 rad/sec².

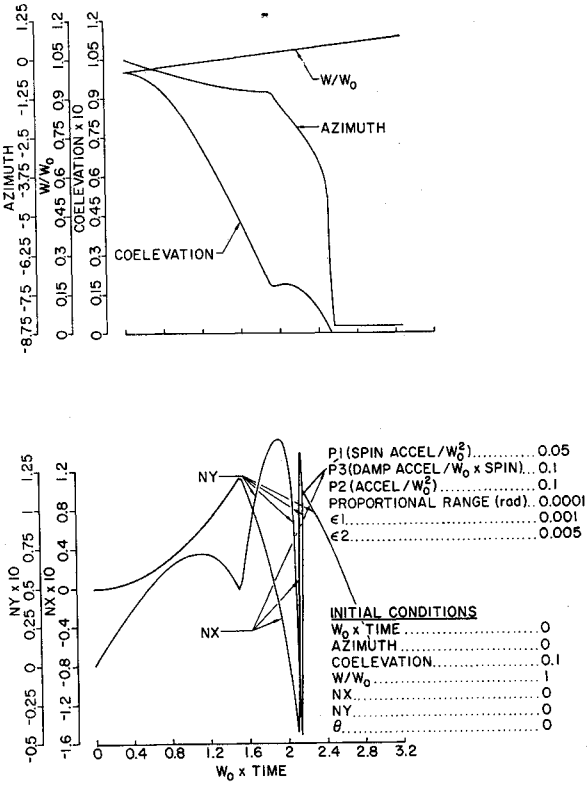

Fig. 9 Results using exact equations ($E_0 = 0.10$).

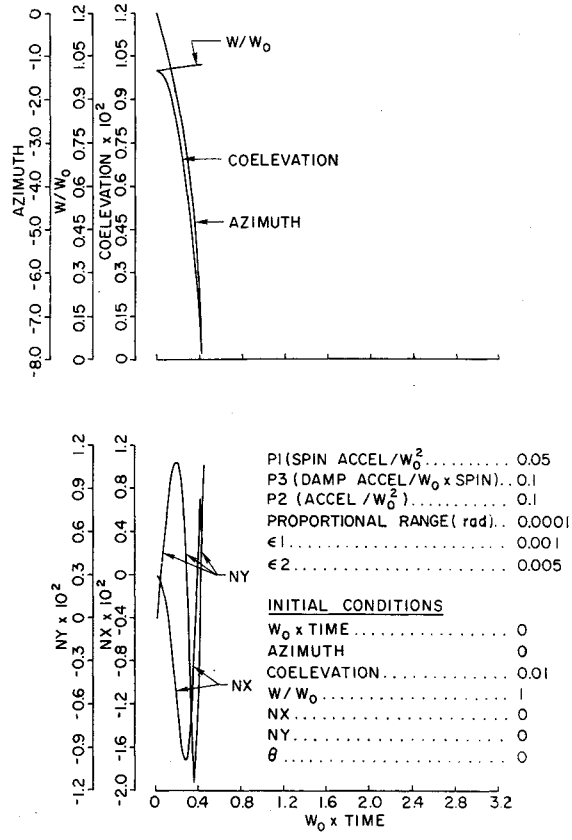

Fig. 10 Results using exact equations ($E_0 = 0.01$).

$P_2 \leq 0.1$; erection would be started at 3.5 sec and completed by 41.3 sec.) (These solutions do not include the time for fine erection; although it turns out that this is small, it should be included.)

E. Results for Hemispheric Torquing

1. *Exact equations*

Because of long digital integration times, the results for the exact equations are samples of the solution for various initial conditions. Three samples are illustrated in Figs. 8–10. The parameters used were

$$P_1 = 0.05,\ P_2 = 0.10,\ P_3 = 0.10$$

proportional range = 0.0001 rad

$$\epsilon_1 = 0.001;\ \epsilon_2 = 0.005$$

The plot with the initial $E = 2.0$ radians (Fig. 8) illustrates the ability of the hemispheric torquer to move the rotor z axis towards the desired spin axis even when it is initially upside down. The other plots, Figs. 9 and 10, also illustrate the ability to drive coelevation to zero. The transients in N_x and N_y which cause the long digital integration times are apparent on all three figures. Roughly 100 digital solutions to the exact equations have been sampled. All solutions behaved properly in the sense that coelevation (E) decreased.

2. *Results using KB approximation*

With the improved speed using the KB equations, several families of curves for coelevation vs time could be determined. Figure 11 shows these results for a typical case, which agree quite closely with the slightly less accurate analytical approximations. See Ref. 7 for more details. The ellipticity terms were intentionally omitted; for reasonable values ($\epsilon \leq 10^{-3}$) they will not materially affect the results.

3. *Experimental results*

The hemispheric torquer has been operated with an air-bearing gyro with switching electronics designed at Stanford. Hemispheric coding has been applied and successfully run. The method of hemispheric torquing has demonstrated its ability to erect through angles greater than 90° in this experiment.

On the basis of these derivations and results, the following can be stated:

1) All results show that the method of hemispheric torquing works.

2) Since $N_{x0} = [P_2(2/\pi)]/(1 + P_1\tau)^2$, and N_{x0} should be small, P_2 is restricted to be less than 0.1. (This restriction is removed in practice with active spin caging.)

3) Figure 6 shows that P_2/P_1 ratios of less than 2 lead to damping times that are quite long (for the worst case). Ratios greater than 2 are usually restricted from a heating standpoint, that is $K_2^2 + K_1^2$ has an upper limit that is a function of how much heat is tolerable. A ratio in the range 1.5 to 2.0 seems to be best.

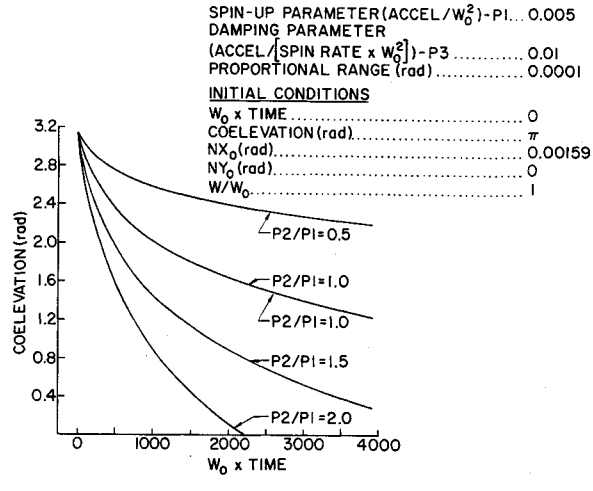

Fig. 11 Results of KB approximation ($P_1 = 0.005$).

4) With active caging of the spin vector along the case x-axis, it was possible to turn on the hemispheric torquor simultaneously with the spin torque. This usually resulted in much faster erection times than those indicated by Fig. 6.

Summary

The technique of active damping by hemispheric torquing results in much shorter ready times than other methods of damping free-rotor gyros. The experimentation that has been done with an air-bearing model indicates that the increased electronics complexity necessary to realize the method is small. The experiments with the model have successfully shown the ability of the gyro to completely invert the spin axis in the rotor automatically.

Although not presented here, fine damping using the optical flat has been shown to be mathematically feasible. The fine damping using a "D pattern" readout was not discussed, but has been done.

The expected reduction in damping time using active damping is at least of the order of 90%, and it is possible to design the system such that damping is completed simultaneously with spin-up.

References

[1] Lange, B., "The Unsupported Gyroscope," presented at the Unconventional Inertial Sensors Symposium, New York, Nov. 1964.

[2] Lange, B., "The Drag-Free Satellite," *AIAA Journal*, Vol. 2, No. 9, Sept. 1964, p. 1590.

[3] Lange, B. O., Fleming, A. W., and Parkinson, B. W., "Control Synthesis for Spinning Aerospace Vehicles Via the Property of 'Frequency Symmetry,'" *Journal of Spacecraft and Rockets*, Vol. 4, No. 2, pp. 142–150.

[4] Lange, B. O. and Fleming, A. W., "The Control of Linear Constant Dynamical Systems Which Are 'Frequency Symmetric' But Not 'Complex Symmetric,'" Paper 33A, Session 33, *Proceedings of the 1966 Congress of the International Federation of Automatic Control*, London, England, June 1966, pp. 33A. 1–33 A 12.

[5] Kryloff, N. and Bogoliuboff, N., *Introduction to Non-Linear Mechanics*, translated by S. Lefschetz, Princeton Univ. Press, Princeton, N.J., 1947.

[6] Fleming, A. W., "The Use of the Properties of Frequency Symmetry and Complex Symmetry in the Control of Linear Dynamical Systems," Ph.D. dissertation, Dept. of Aeronautics and Astronautics, Stanford Univ., Stanford, Calif.; also SUDAAR Rept. 266.

[7] Parkinson, B. W., "The Active Damping of Free Rotor Gyros," Ph.D. dissertation, May 1966, Dept. of Aeronautics and Astronautics, Stanford Univ., Stanford, Calif.; also SUDAAR Rept. 260.

JUNE 1970 J. SPACECRAFT VOL. 7, NO. 6

Experimental Studies of the Active Damping of Free-Rotor Gyroscopes

BRADFORD W. PARKINSON*
U. S. Air Force Academy, Colorado Springs, Colo.

AND

BENJAMIN O. LANGE†
Stanford University, Stanford, Calif.

This paper reports the experimental studies of a previously analyzed method of active damping of the nearly spherical rotor of a free-rotor gyro. The rotor must be damped (after spin-up) to spin about its axis of maximum inertia if rotor-fixed markings are used for readout. Both coarse ("hemispheric torquing") and fine active damping have been mechanized in an air-bearing gyro. The experimental damping characteristics agree well with the theoretical results and show that 1) damping to an accuracy of a few arc seconds can be completed in the same amount of time required to bring the rotor to operating speed, and 2) it can be accomplished so that the same side is always up, thus eliminating the necessity for the choice between two error models for the gyro or multiple start-up attempts until the correct side is up.

Nomenclature

E = coelevation angle between angular velocity vector of the rotor and the desired spin axis
h_μ, h_σ = lengths defined in Fig. 5
I_z = z axis moment of inertia
i_x = rms current in X or Y coil
i_{zx},i_{zy} = rms current in Z coil in quadrature with the X coil and the Y coil, respectively
K_m = experimentally determined coefficient giving torque/(amp)^2
K_p = polhode damper loop gain (cf. Ref. 2, p. 90)
K_δ = spin caging torque
k = l, V_{zy}/V, and V_{zx}/V for z, y, and x torques, respectively
L = coefficient of air drag resistance
$\mathbf{M}^+$,$\mathbf{M}^-$ = positive and negative torques, respectively
$\mathbf{M}_d$,$\mathbf{M}_e$ = disturbing and erection torques, respectively
$\mathbf{M}_h$ = undesired disturbing torque
$\mathbf{M}_{ht}$ = torquing signal from hemispheric torquer
$\mathbf{M}_{\max}$ = peak value of the torque
$\mathbf{M}_x$,$\mathbf{M}_y$,$\mathbf{M}_z$ = case x, y, and z axis torques, respectively
$\mathbf{M}_{xb}$,$\mathbf{M}_{xi}$ = average values of the torques along the x axis in the rotor and the x axis in the case, respectively

Received August 2, 1967; presented as Paper 67-590 at the AIAA Guidance, Control, and Flight Dynamics Conference, Huntsville, Ala., August 14–16, 1967; revision received September 29, 1969. The research reported here is part of a program supported at Stanford University by the U.S. Air Force under Contract AF33(615)-1411 from the Air Force Avionics Laboratory and is part of B. Parkinson's doctoral thesis.

* Member of Faculty, Department of Astronautics and Computer Science; Lt. Colonel, U.S. Air Force. Member AAIA.

† Associate Professor, Department of Aeronautics and Astronautics. Member AAIA.